

1 Arrangement techniques of proteins and cells using
2 amorphous calcium phosphate nanofiber scaffolds
3

4 Takayuki Nonoyama ^a, Takatoshi Kinoshita ^{a*}, Masahiro Higuchi ^b, Kenji Nagata ^b,
5 Masayoshi Tanaka ^a, Mari Kamada ^c, Kimiyasu Sato ^d, Katsuya Kato ^{d*}

6 ^a *Department of Frontier Materials, Graduate School of Engineering, Nagoya Institute*
7 *of Technology, Gokisho-cho, Showa-ku, Nagoya, Aichi, 466-8555, Japan*

8 ^b *Department of Materials Science and Engineering, Graduate School of Engineering,*
9 *Nagoya Institute of Technology, Gokisho-cho, Showa-ku, Nagoya, Aichi, 466-8555,*
10 *Japan*

11 ^c *Division of Chemistry for Materials, Graduate School of Engineering,*
12 *Mie University, 1577 Kurimamachiya-cho, Tsu, Mie 514-8570, Japan*

13 ^d *National Institute of Advanced Industrial Science and Technology (AIST), 2266-98*
14 *Anagahora, Shimo-Shidami Moriyama-ku, Nagoya, Aichi, 463-8560, Japan*

15
16 Corresponding Author

17 *Phone: +81-52-735-5267, Fax: +81-52-735-5267,*

18 *E-mail address: kinoshita.takatoshi@nitech.ac.jp (Prof. T. Kinoshita)*

19 *Phone: +81-52-736-7551, Fax: +81-52-736-7405,*

20 *E-mail address: katsuya-kato@aist.go.jp (Dr. K. Kato)*
21

1 **ABSTRACT**

2 We demonstrate arrangement techniques of proteins and cells using an amorphous
3 calcium phosphate (ACP) nanofiber scaffold. It is well known that protein and
4 osteoblastic cell are preferably adsorbed onto ACP surface. The ACP nanofiber scaffold
5 was prepared by calcium phosphate mineralization on a polypeptide monolayer-coated
6 mica substrate, and ACP nanofibers were oriented unidirectionally. In a protein system,
7 the ACP nanofiber scaffold was soaked in a fluorescein isothiocyanate conjugated
8 immunoglobulin G (IgG-FITC) aqueous solution. From fluorescence microscopic
9 measurement, the adsorbed IgG-FITC was highly confined and arranged on the ACP
10 nanofiber. In a cell system, a mouse osteoblast-like cell (MC3T3-E1) behavior on the
11 ACP nanofiber scaffold was observed. The cell was elongated unidirectionally, and its
12 cytoskeletal shape showed high aspect ratio. These results are clearly different from an
13 ACP bulk template or bare mica substrate, and the arrangement technique enable to
14 fabricate a fine-tuned biomaterial template.

15

16 ***Keywords:***

17 Arrangement technique, Osteoblast-like cell, Antibody protein, Mineralization,
18 β -Sheet peptide template, Amorphous calcium phosphate

19

20

21

1 **1. Introduction**

2 An arrangement technique of cells and proteins has potential for the development of
3 tissue engineering and bio-sensing tools. In nature, a cell is the smallest unit of living
4 organism, and macro anatomies such as organ and muscle are formed by cellular
5 orientation and organization. Thus, we believe that the arrangement technique of
6 biomaterials will be a technological bridge between and artificial (experimental) stage
7 and a natural (functional) stage in the tissue engineering. The protein orientational
8 technique has been researched for a bio-sensing using peptide, enzyme, antibody and
9 polysaccharide [1-10]. The tissue engineering materials whose surface enable to
10 assemble cells have advantage in bone-repairing ability.

11 In previous studies, it is clear that the cell recognizes surface geometry, and
12 scaffold's surface characteristics control the cell behavior. A human gingival fibroblast
13 cell adheres and orients along the groove direction of a titanium scaffold and also
14 recognizes the difference of surface roughness [11]. Such contact guidance phenomenon
15 is commonly noted about various cells [12-16], therefore, cell's adhesion, extension,
16 propagation and orientation can be control with a surface-fabricated template. In
17 addition, it is well known that a surface chemistry also controls the cell behavior
18 [17-19]. Keselowsky et al. showed the cell adhesion on various functional
19 group-modified templates [20]. A mouse osteoblast-like MC3T3-E1 cell adhere well on
20 hydroxyl groups-modified surface more than other functional group-modified ones such
21 as carboxyl, amino and methyl groups. Also, the cell behavior is related to a substrate's

1 crystal phase. An osteoblast cell adsorption onto several crystal phases of calcium
2 phosphate was investigated to simulate the bone regeneration system [21-24]. An
3 amorphous calcium phosphate (ACP) surface has highly cell adhesion ability more than
4 hydroxyapatite (HA) one. Although the ACP surface is great successful, its amorphous
5 phase is very unstable, and the ACP morphology is hard to control.

6 In our previous work, we produced the unidirectional ACP nanofiber scaffold by
7 peptide-based biomineralization [25,26]. We prepared the β -sheet conformational
8 peptide nanofiber on the mica substrate and applied the calcium phosphate
9 mineralization onto this peptide template. Although the ACP is unstable and does not
10 grow anisotropically in general, stable ACP nanofibers were formed on our peptide
11 template. Therefore, the ACP nanofiber template is ideal scaffold to establish the
12 fundamental arrangement technique of proteins and cells.

13 In this study, we present adsorption behaviors of immunoglobulin G (IgG) and
14 mouse osteoblast-like cell (MC3T3-E1) onto the ACP nanofiber scaffold, respectively.
15 We also investigate the adsorption onto ACP bulk scaffold, bare mica plate and peptide
16 monolayer template as control experiments and show the advantage of the ACP
17 nanofiber scaffold as the template for arrangement techniques of proteins and cells.

18

19 **2. Experimental Section**

20 *2.1 Preparation of ACP Nanofiber Template*

21 We prepared the ACP nanofiber template by calcium phosphate mineralization on the

1 peptide monolayer (Scheme 1). In our previous study, we succeeded to fabricate a
2 monolayer template of orientational peptide nanofibers [25-26]. This peptide has
3 hydrophobic leucine (L) – hydrophilic glutamic acid (E) alternate sequence (LE)₈ that is
4 easy to form a β -sheet conformation, moreover, polyethylene glycol (PEG, degree of
5 polymerization = 70) is placed at the C-terminal of (LE)₈ to prevent a formation of
6 amyloid-like aggregate. Therefore, this peptide was named (LE)₈-PEG₇₀ and
7 synthesized by combinatorial solid phase peptide synthesis [27]. Dipping the fresh mica
8 substrate in 1.0×10^{-5} M (LE)₈-PEG₇₀ aqueous solution (pH 11.0) at 25 °C for 18 h,
9 peptides adsorb on the mica surface and self-assemble to unidirectional nanofibers. On
10 this peptide monolayer template, we carried out the calcium phosphate mineralization
11 by what we call the alternate dropping method. For the calcium and phosphate sources,
12 we used aqueous solutions of calcium acetate (Ca(CH₃COO)₂) and diammonium
13 hydrogen phosphate ((NH₄)₂HPO₄). 20 μ L of a 50 mM Ca(CH₃COO)₂ aq solution was
14 dropped onto the peptide-template over the course of 1 min. Then, the template was
15 rinsed and dried. The washing process removes the surplus calcium ions on the peptide
16 surface and prevents homogeneous nucleation when the phosphate source is dropped.
17 Then, 20 μ L of a 30 mM (NH₄)₂HPO₄ aq solution was dropped onto the template in the
18 same way. After 10 min, the template was washed and dried again. An ACP bulk
19 template as a control was prepared by alternate soaking method that bare mica substrate
20 was soaked in 50 mM Ca(CH₃COO)₂ aq and 30 mM (NH₄)₂HPO₄ aq solutions
21 alternately.

1

2 *2.2 Protein Adsorption*

3 Protein orientational adsorption was carried out on the ACP nanofiber template. First,
4 to confirm that proteins could adsorb and orient on ACP nanofiber, IgG-FITC
5 adsorption was applied. The ACP nanofiber scaffold was soaked in 0.5 or 0.05 wt%
6 IgG-FITC aqueous solution for 1 h. After adsorption, the template was rinsed with
7 distilled water to remove surplus adsorbed IgG-FITC. The ACP bulk scaffold, bare
8 mica substrate and peptide monolayer template were used as control experiments.
9 Second, to better the MC3T3-E1 cell adhesion onto the template, fibronectin that is
10 commonly known as an adhesive protein of cells was adsorbed on the ACP nanofiber
11 scaffold. The template was soaked in 0.05 or 0.5 wt% fibronectin aqueous solution and
12 incubated at 37 °C under 5 % CO₂ atmosphere for 2 h. After incubation, the template
13 was rinsed with phosphate-buffered saline (PBS (-)).

14

15 *2.3 Cell Culture*

16 Mouse osteoblast-like cell MC3T3-E1 (Riken Bio Research Center, Japan) was
17 cultured in the minimum essential alpha medium (α -MEM) containing 10wt% fetal
18 bovine serum (FBS) and 1wt% penicillin-streptomycin. During the cell culturing, the
19 experimental system was maintained in 5% CO₂ at 37 °C using a gas jacket incubator.
20 The MC3T3-E1 cell was trypsinized and 3 mL of a suspension (5.0×10^3 cells/cm²) was
21 added to each template placed into the well of a 6-wells plate. Templates of ACP

1 nanofiber, ACP bulk, bare mica and peptide monolayer were incubated for 24 h under
2 standard culture conditions (5% CO₂, 37 °C), respectively. After incubation, the
3 suspension was removed, and cells were rinsed with PBS (-) and were fixed with 3.7%
4 formaldehyde in PBS (-) for 10 min. The fixed cell membrane was permeabilized with
5 0.1% Triton-X-100-containing PBS (-) at room temperature for 5 min and incubated
6 with 400 μL PBS (-) containing 10 μL rhodamine-phalloidin, 1% arubuminn for 20 min
7 to stain the actin filament. We observed the IgG-FITC protein and the actin filament
8 stained with rhodamine-phalloidin by fluorescence microscope (BX51, OLYMPUS Co.
9 Japan).

10

11 **3. Results and Discussion**

12 *3.1 Morphology of ACP Nanofiber Scaffold*

13 We show the field-emission scanning electron microscopic (FE-SEM) image of the
14 ACP nanofiber scaffold in Fig. 1. Unidirectional nanofibers were observed on the
15 peptide-coated mica surface and formed at regular intervals. Formation of the
16 orientational morphology relates to the peptide monolayer that consists of β-sheet
17 nanofibers. At the outermost layer of the peptide monolayer, carboxyl groups that are
18 side chain of glutamic acid orient two-dimensionally and induce the calcium phosphate
19 mineralization. Therefore, the calcium phosphate precipitation which cannot be
20 normally controlled their morphology is confined by the orientational peptide
21 monolayer. The crystal phase of the calcium phosphate nanofiber was ACP assigned by

1 electron diffraction measurement [25].

2

3 *3.2 Protein Adsorption*

4 The ACP nanofiber, ACP bulk, bare mica and peptide monolayer templates that were
5 soaked in the 0.05 wt% IgG-FITC aqueous solution were observed by fluorescence
6 microscopy, respectively (Fig. 2). On the ACP nanofiber scaffold, highly confined and
7 oriented adsorption of IgG-FITC protein was observed along the ACP nanofiber
8 direction (a : fluorescence image, f : optical image). On the other hand, IgG-FITC was
9 adsorbed randomly on the ACP bulk scaffold (b), bare mica substrate (c) and peptide
10 template (d) as the control experiments. On the ACP nanofiber fiber template, the
11 peptide monolayer was exposed between the ACP nanofibers. At the surface of peptide
12 monolayer, the PEG part that is inhibitor of protein adsorption is also exposed [28-30].
13 Moreover, calcium phosphate generally has highly protein-adsorbed ability and is used
14 as a protein adsorbent reagent [31,32]. Therefore, the IgG-FITC was selective adsorbed
15 onto the ACP parts. IgG was able to adsorb onto the mica surface because mica surface
16 also had hydrophilic group such as hydroxyl group. At the result of 0.5 wt%
17 solution-treated to ACP nanofiber template, IgG-FITC was adsorbed randomly (e).
18 Therefore, the ACP part reached critical limit to adsorb the protein, and IgG was also
19 adsorbed onto the peptide monolayer region.

20

21 *3.3 Cell Adhesive Behavior*

1 The MC3T3-E1 cell adhesion was applied onto ACP nanofiber, ACP bulk, peptide
2 monolayer and bare mica templates, respectively, and their
3 rhodamine-phalloidin-stained actin filaments were observed by fluorescence
4 microscopy (Fig. 3). On ACP nanofiber (a) and peptide monolayer templates (b), actin
5 stress fibers elongated anisotropically, respectively. Especially, the actin fibers on the
6 ACP fiber template were longer than on the peptide template (average of filament
7 length, on ACP nanofiber: $430\pm 12\ \mu\text{m}$; on peptide monolayer: $332\pm 7\ \mu\text{m}$) and were
8 highly aspect ratio (on ACP nanofiber: 50.2; on peptide monolayer: 32.4). It is well
9 known that the MC3T3-E1 adhesion is promoted on ACP surface [33]. At the outermost
10 surface of ACP, calcium ion may elute slowly, and Ca^{2+} concentration is locally
11 increased at the scaffold's surface. These calcium ions promote a cellular motor protein
12 such as myosin, which is driven with energy of adenosine triphosphate hydrolysis.
13 Comparing ACP bulk and bare mica templates, although the cell's extensional direction
14 was not controlled, the stress fiber was also more elongated on the ACP bulk template
15 than on the bare mica substrate. From the viewpoints of the surface geometry and
16 chemistry, ACP nanofiber scaffold is ideal template to control the cell orientation. To
17 better the cell adhesion, we additionally immobilized the fibronectin that is adhesive
18 protein on the ACP nanofiber. Fig. 4 shows the actin filament of M3CT3-E1 on 0.05
19 wt% (a) and 0.5 wt% (b) fibronectin solution-treated ACP nanofiber scaffolds. As the
20 fibronectin concentration was increased, the number of cell was increased, but the
21 filament length and aspect ratio were decreased. Fibronectin was adsorbed enough on

1 both the ACP fiber parts and non-ACP parts (peptide part) at 0.5 wt%. Therefore,
2 surface specific pattern was buried, and cells were omnidirectionally elongated.

3

4 **4. Conclusion**

5 We demonstrate the arrangement techniques of protein and cell on our ACP
6 nanofiber scaffold. Both IgG protein and MC3T3-E1 osteoblast-like cell were attached
7 well along the ACP nanofiber direction, and these results were clearly different against
8 their behaviors on peptide monolayer and bare mica substrate. At the present, we are
9 able to fabricate various morphological calcium phosphate nano-patterned scaffolds, in
10 addition, the nanofiber consisted of hydroxyapatite crystal phase is also prepared on the
11 various kinds of peptide monolayers. The peptide monolayer controls the calcium
12 phosphate crystal phase and morphology. Therefore, we believe that protein and cell
13 orientational systems that enable to comply the various needs in the fields of tissue
14 engineering and bio-sensing technology will be produced using this technique.

15

16 **Acknowledgements**

17 This work was partly supported by Grant-in-Aid for Scientific Research (C)
18 No.23560925 from Japan Society for the Promotion of Science (JSPS). We
19 acknowledge the support of the SER program from the Institute of Ceramics Research
20 and Education (ICRE) administered by Nagoya Institute of Technology (Prof. T.
21 Kasuga and Prof. Y. Iwamoto).

1

2

3 **References**

4 (1) A. M. Samoylov, T. I. Samoylova, S. T. Pathirana, L. P. Globa, V. J. Vodyanoy,
5 Peptide biosensor for recognition of cross-species cell surface markers, *J. Mol. Recognit.*
6 15 (2002) 197-203.

7 (2) M. Yemini, M. Reches, E. Gazit, J. Rishpon, Peptide nanotube-modified
8 electrodes for enzyme-biosensor applications, *Anal. Chem.* 77 (2005) 5155-5159.

9 (3) E. Mateo-Martí, C. Briones, C. M. Pradier, J. A. Martín-Gago, A DNA biosensor
10 based on peptide nucleic acids on gold surfaces, *Biosens. Bioelectron.* 22 (2007)
11 1926-1932.

12 (4) K. Enander, L. Choulier, A. L. Olsson, D. A. Yushchenko, D. Kanmert, A. S.
13 Klymchenko, A. P. Demchenko, Y. Mély, D. Altschuh, A peptide-based, ratiometric
14 biosensor construct for direct fluorescence detection of a protein analyte, *Bioconjugate*
15 *Chem.* 19 (2008) 1864-1870.

16 (5) G. S. Wilson, Y. Hu, Enzyme-based biosensors for in vivo measurements, *Chem.*
17 *Rev.* 100 (2000) 2693-2704.

18 (6) E. Katz, A. F. Bückmann, I. Willner, Self-powered enzyme-based biosensors, *J.*
19 *Am. Chem. Soc.* 123 (2001) 10752-10753.

20 (7) B. Hock, M. Seifert, K. Kramer, Engineering receptors and antibodies for
21 biosensors, *Biosens. Bioelectron.* 17 (2002) 239-249.

- 1 (8) R. Jelinek, S. Kolusheva, Carbohydrate biosensors, Chem. Rev. 104 (2004)
2 5987-6015.
- 3 (9) M. Chikae, T. Fuku, K. Kerman, K. Idegami, Y. Miura, E. Tamiya, Amyloid- β
4 detection with saccharide immobilized gold nanoparticle on carbon electrode,
5 Bioelectrochemistry 74 (2008) 118-123.
- 6 (10) M. Higuchi, T. Koga, K. Taguchi, T. Kinoshita, Substrate-induced conformation
7 of an artificial receptor with two receptor sites, Langmuir 18 (2002) 813-818.
- 8 (11) T. Inoue, J. E. Cox, R. M. Pilliar, A. H. Melcher, Effect of the surface geometry
9 of smooth and porous-coated titanium alloy on the orientation of fibroblasts in vitro, J.
10 Biomed. Mater. Res. Part A 21 (1987) 107-126.
- 11 (12) P. Clark, P. Connolly, A. S. Curtis, J.A. Dow, C. D. Wilkinson, Topographical
12 control of cell behaviour. I. Simple step cues, Development 99 (1987) 439-448.
- 13 (13) J. Meyle, K. Gültig, W. Nisch, Variation in contact guidance by human cells on
14 a microstructured surface, J. Biomed. Mater. Res. Part A 29 (1995) 81-88.
- 15 (14) J. A. Alaerts, V. M. De Cuperea, S. Mosera, P. van den Bosh de Aguilarb, P. G.
16 Rouxhet, Surface characterization of poly(methyl methacrylate) microgrooved for
17 contact guidance of mammalian cells, Biomaterials 22 (2001) 1635-1642.
- 18 (15) E. K. F. Yim, R. M. Reano, S. W. Pang, A. F. Yee, C. S. Chen, K. W. Leong,
19 Nanopattern-induced changes in morphology and motility of smooth muscle cells,
20 Biomaterials 26 (2005) 5405-5413.
- 21 (16) J. Sun, Y. Ding, N. J. Lin, J. Zhou, H. Ro, C. L. Soles, M. T. Cicerone, S. L.

1 Gibson, Exploring cellular contact guidance using gradient nanogratings,
2 *Biomacromolecules* 11 (2010) 3067-3072.

3 (17) A. J. García, M. D. Vega, D Boettiger, Modulation of cell proliferation and
4 differentiation through substrate-dependent changes in fibronectin conformation, *Mol.*
5 *Biol. Cell* 10 (1999) 785-798.

6 (18) L. T. Allen, E. J. P. Fox, I. Blute, Z. D. Kelly, Y. Rochev, A. K. Keenan, K. A.
7 Dawson, W. M. Gallagher, Interaction of soft condensed materials with living cells:
8 Phenotype/transcriptome correlations for the hydrophobic effect, *Proc. Natl. Acad. Sci.*
9 *USA* 100 (2003) 6331-6336.

10 (19) M. Mrksich, A surface chemistry approach to studying cell adhesion, *Chem. Soc.*
11 *Rev.* 29 (2000) 267-273.

12 (20) B. G. Keselowsky, D. M. Collard, A. J. García, Surface chemistry modulates
13 fibronectin conformation and directs integrin binding and specificity to control cell
14 adhesion, *J. Biomed. Mater. Res. Part A* 66A (2003) 247-259.

15 (21) S. Guido, R. T. Tranquillo, A methodology for the systematic and quantitative
16 study of cell contact guidance in oriented collagen gels Correlation of fibroblast
17 orientation and gel birefringence, *J. Cell Sci.* 105 (1993) 317-331.

18 (22) N. Masahisa, N. Takashi, K. Tadashi, T. Masami, O. Masaki, Differences of
19 bone bonding ability and degradation behavior in vivo between amorphous calcium
20 phosphate and highly crystalline hydroxyapatite coating, *Biomaterials* 17 (1996) 1771-
21 1777.

- 1 (23) D. Tadic, F. Peters, M. Epple, Continuous synthesis of amorphous carbonated
2 apatites, *Biomaterials* 23 (2002) 2553-2559.
- 3 (24) J. S. Sun, Y. H. Tsuang, C. J. Liao, H. C. Liu, Y. S. Hang, F. H. Lin, The effects
4 of calcium phosphate particles on the growth of osteoblasts, *J. Biomed. Mater. Res. Part*
5 *A* 37 (1997) 324-334.
- 6 (25) T. Nonoyama, M. Tanaka, T. Kinoshita, F. Nagata, K. Sato, K. Kato,
7 Morphology control of calcium phosphate by mineralization on the β -sheet peptide
8 template, *Chem. Commun.* 46 (2010) 6983-6985.
- 9 (26) T. Nonoyama, T. Kinoshita, M. Higuchi, K. Nagata, M. Tanaka, K. Sato, K.
10 Kato, Multistep growth mechanism of calcium phosphate in the earliest stage of
11 morphology-controlled biomineralization, *Langmuir* 27 (2011) 7077-7083.
- 12 (27) G. B. Fields, R. L. Noble, Solid phase peptide synthesis utilizing
13 9-fluorenylmethoxycarbonyl amino acids, *Int. J. Pept. Protein Res.* 35 (1990) 161-214.
- 14 (28) S. I. Jeon, J. H. Lee, J. D. Andrade, P. G. de Gennes, Protein-surface
15 interactions in the presence of polyethylene oxide, *J. Colloid Interface Sci.* 142 (1991)
16 149-166.
- 17 (29) R. Israëls, F. A. M. Leermakers, G. J. Fleer, Adsorption of charged block
18 copolymers: Effect on colloidal stability, *Macromolecules* 28 (1995) 1626-1634.
- 19 (30) M. Björling, Interaction between surfaces with attached poly(ethylene oxide)
20 chains, *Macromolecules* 25 (1992) 3956-3970.
- 21 (31) A. Tiselius, S. Hjertén, Ö. Levin, Protein chromatography on calcium phosphate

1 columns, Arch. Biochem. Biophys. 65 (1956) 132-155.

2 (32) J. M. Thomann, M. J. Mura, M. S. Behr, J. D. Aptel, A. Schmitt, E. F. Bres, J. C.
3 Voegel, Adsorption kinetics of human plasma albumin on negatively charged
4 hydroxyapatites. Surface charge effects, Colloids Surf. 40 (1989) 293-305.

5 (33) G. Balasundaram, M. Sato, T. J. Webstera, Using hydroxyapatite nanoparticles
6 and decreased crystallinity to promote osteoblast adhesion similar to functionalizing
7 with RGD, Biomaterials 27 (2006) 2798-2805.

8

9

10

11

12

13

14

15

16

17

18

19

20

21

1

2

3 **Scheme caption**

4 **Scheme 1** Preparation of the ACP nanofiber on the peptide self-assembled-monolayer.

5 (a) β -sheet peptides self-assemble to the nanofiber. (b) Peptide nanofibers self-organize

6 to the monolayer. (c) Calcium ions are trapped and confined by hydroxyl groups of the

7 peptide monolayer surface. (d) Calcium phosphate precipitation is formed along the

8 peptide nanofiber direction.

9

10 **Figure captions**

11 **Figure 1** FE-SEM image of the ACP precipitate on the peptide monolayer. The

12 unidirectional ACP nanofibers were formed along the peptide nanofiber direction.

13 **Figure 2** Fluorescence microscopic images of IgG-FITC adsorbed onto (a) ACP

14 nanofiber scaffold, (b) ACP bulk scaffold, (c) bare mica substrate and (d) peptide

15 monolayer, respectively. Templates were soaked in 0.05 wt% IgG-FITC aq solution. (e)

16 ACP nanofiber scaffold was soaked in 0.5 wt% IgG-FITC aq solution. (f) Optical

17 microscopic image of (a).

18 **Figure 3** Fluorescence microscopic images of rhodamine-phalloidin-stained actin

19 filaments onto (a) ACP nanofiber scaffold, (b) ACP bulk scaffold, (c) bare mica

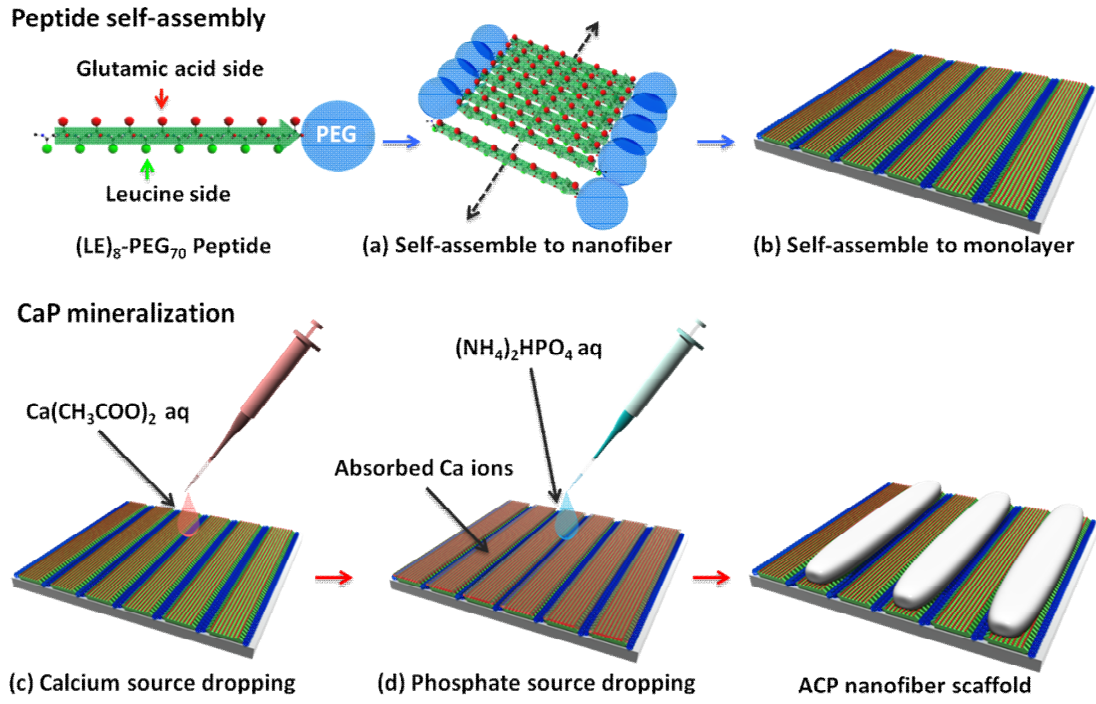
20 substrate and (d) peptide monolayer, respectively.

21 **Figure 4** Dependence of the cell behavior on the fibronectin concentration. The ACP

1 nanofiber scaffolds were soaked in (a) 0.05 wt% and (b) 0.5 wt% fibronectin aqueous
2 solutions at 37 °C under 5% CO₂ atmosphere for 2h. (c) Original ACP nanofiber as the
3 control.

1

Scheme 1



2

3

T. Nonoyama et al.

4

5

6

7

8

9

10

11

12

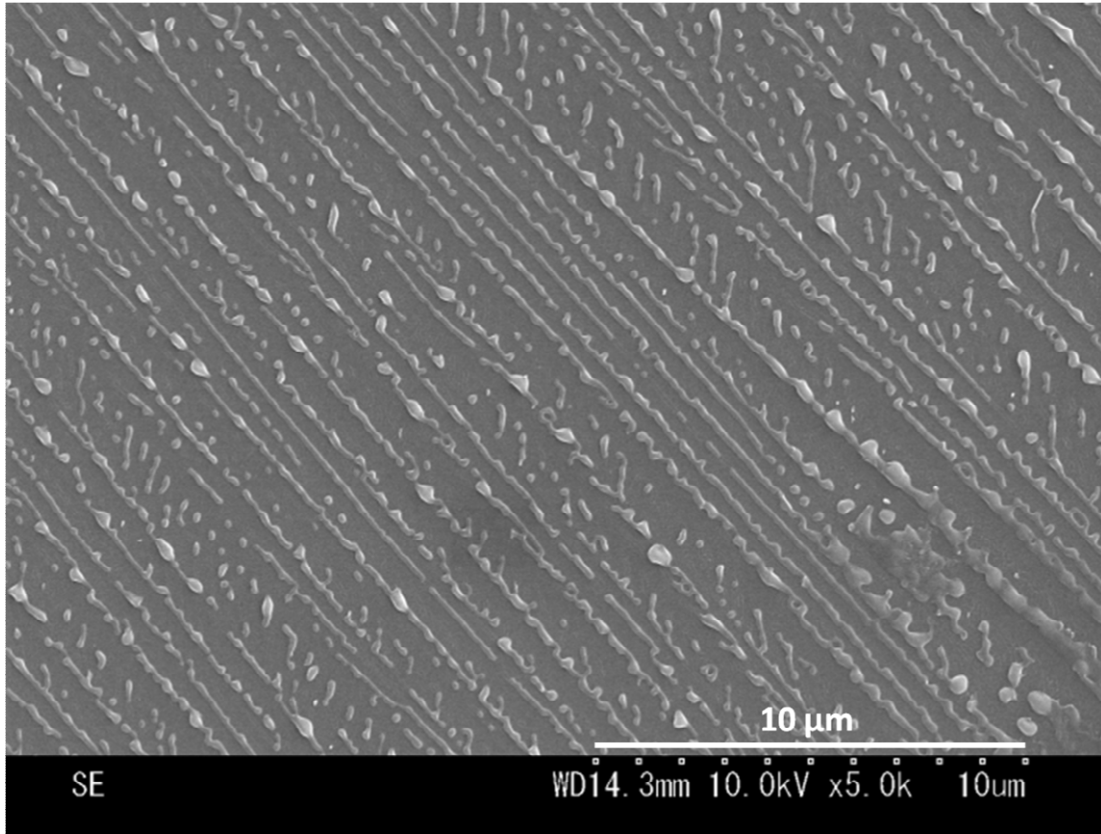
13

1

2

3

Figure 1



4

5

T. Nonoyama et al.

6

7

8

9

10

11

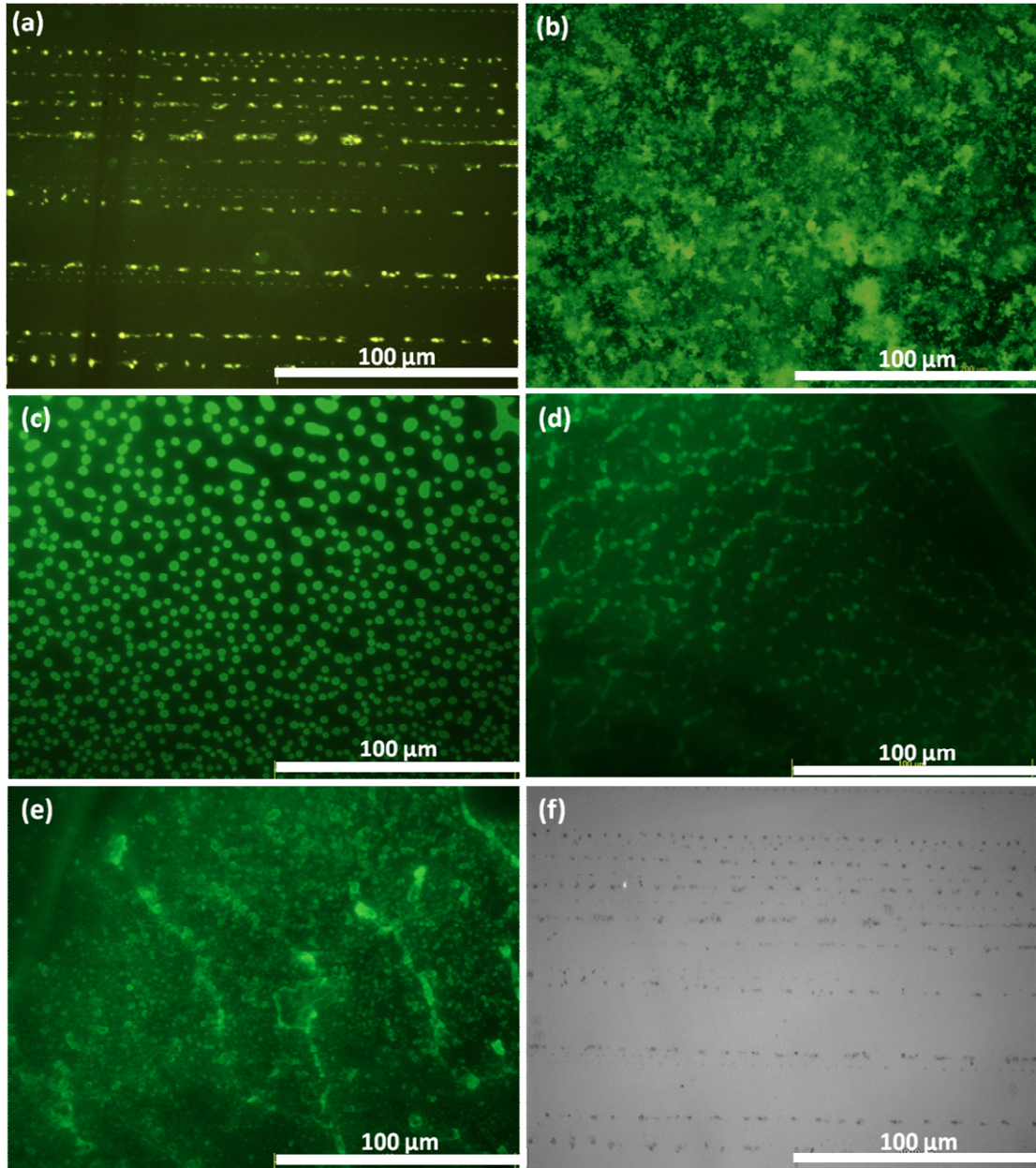
12

1

2

3

Figure 2



4

5

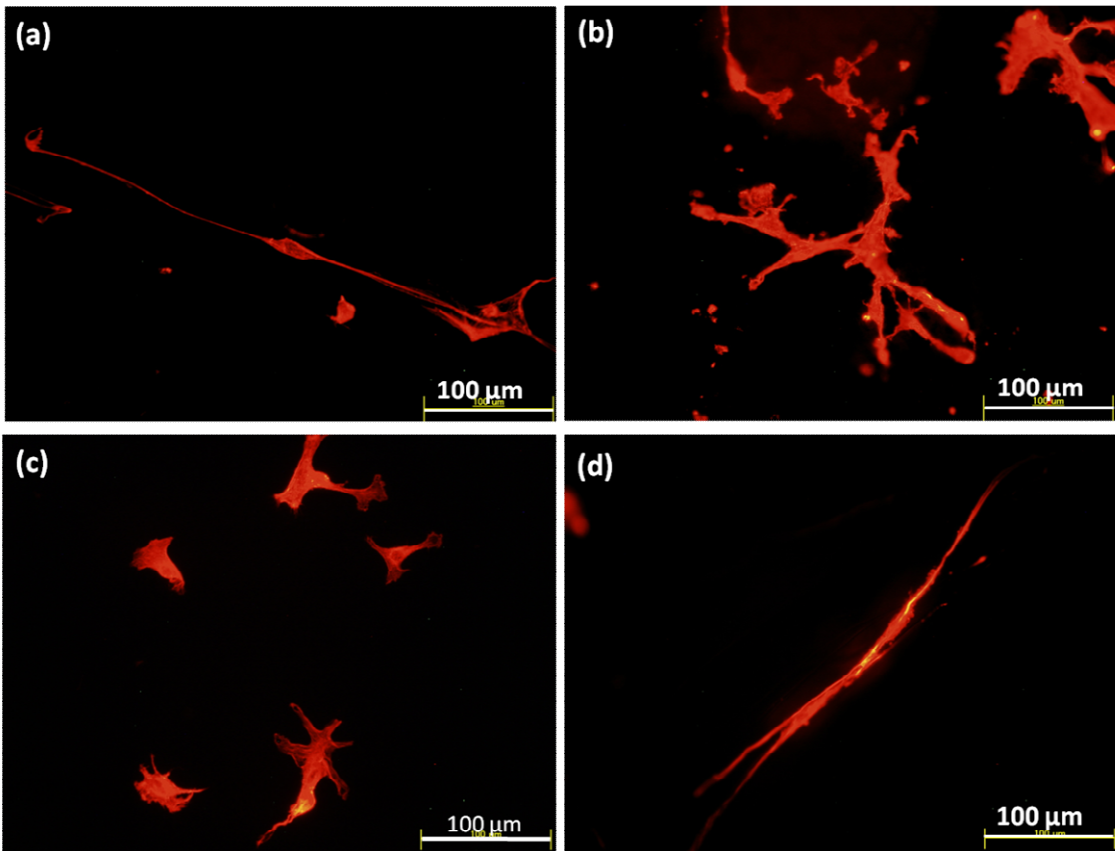
T. Nonoyama et al.

6

7

1
2
3
4
5
6

Figure 3



7
8
9
10
11
12

T. Nonoyama et al.

1

2

3

4

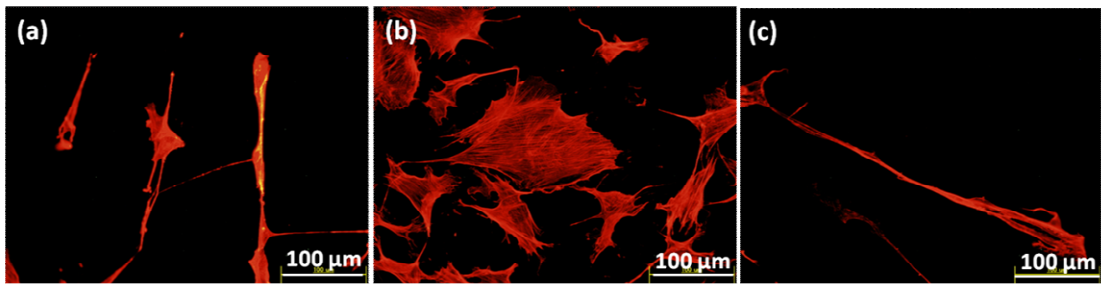
5

6

7

8

Figure 4



9

10

T. Nonoyama et al.

11

12